Eight Years of High Cloud Statistics Using HIRS

DONALD P. WYLIE

Space Science and Engineering Center, University of Wisconsin—Madison, Madison, Wisconsin

W. PAUL MENZEL

Office of Research and Applications, NOAA/NESDIS, Madison, Wisconsin

(Manuscript received 5 September 1997, in final form 13 February 1998)

ABSTRACT

Over the last 8 yr frequency and location of cloud observations have been compiled using multispectral High Resolution Infrared Radiation Sounder (HIRS) data from the National Oceanic and Atmospheric Administration polar-orbiting satellites; this work is an extension of the 4-yr dataset reported by D. Wylie et al. The CO_2 slicing algorithm applied to the HIRS data exhibits a higher sensitivity to semitransparent cirrus clouds than the cloud algorithm used by the International Satellite Cloud Climatology Project; the threshold for cloud detection appears to require visible optical depths (τ_{vis}) greater than 0.1.

The geographical distributions of clouds in the 8-yr dataset are nearly the same as those reported from 4 yr of data. The detection of upper-tropospheric clouds occurs most often in the intertropical convergence zone and midlatitude storm belts with lower concentrations in subtropical deserts and oceanic subtropical highs. The areas of concentrated cloud cover exhibit latitudinal movement with the seasons as in other cloud datasets. HIRS finds clear sky in 25%, opaque cloud in 32%, and semitransparent cloud in 43% of all its observations. The effective emissivity of the all semitransparent clouds ($\tau_{vis} < 6$) ranges from 0.2 to 0.6 with an average value of about 0.5.

Time trends are reexamined in detail. A possible cirrus increase in 1991 reported by Wylie and coauthors in 1994 is found to be diminished upon reinspection. The revised 8-yr record has indications of an increase in high clouds in the northern midlatitudes (0.5% yr^{-1}) but little change elsewhere. The seasonal cycle of cloud cover in the Southern Hemisphere becomes very noticeable in 1993.

1. Introduction

Upper-tropospheric cirrus clouds continue to be the focus of many efforts estimating the role of clouds in the earth's radiation budget. Global studies have been made with satellites (Gruber and Chen 1988; Stowe et al. 1988) and surface weather observations (Warren et al. 1986, 1988). A larger and more comprehensive study is under way with the International Satellite Cloud Climatology Project (ISCCP; Rossow and Schiffer 1991). These studies have relied primarily on data from the 0.7- and 11-μm window channel sensors, which have difficulty identifying optically thin upper-tropospheric clouds. Recently more sensitive methods for detecting upper-tropospheric clouds have been demonstrated using several infrared channels on atmospheric sounding instruments (Chahine 1974; Smith et al. 1974; McCleese and Wilson 1976; Smith and Platt 1978; Wielicki and Coakley 1981; Wylie and Menzel 1989; Menzel et al. 1992; Wylie et al. 1994; Susskind et al. 1997). The infrared channels from 13 to 15 μm, which are on all of the weather satellites operated by the United States, provide a means of detecting optically thin clouds and estimating their density that is more sensitive than techniques using only the visible and infrared window channels. This paper reports on an ongoing investigation of upper-tropospheric clouds using the High resolution Infrared Radiation Sounder (HIRS), which is flown on the polar-orbiting National Oceanic and Atmospheric Administration (NOAA) satellites. Eight years of HIRS observations of clouds have been collected. Wylie et al. (1994) describe the frequency, geographical distribution, and seasonal changes of observations of upper-tropospheric clouds over 4 years (1989–93). That work has been continued using succeeding satellites in the NOAA operational series. This paper presents the statistics of the cloud observations of *NOAA-10, -11, -12,* and *-14* from 1989 through 1997. The frequency of HIRS detection of cloud is referred to as the probability of cloud occurrence; the percentage of cloud cover is inferred from the cloud density (with adjustments for the size of the HIRS field of view).

Corresponding author address: Donald P. Wylie, Space Science and Engineering Center, University of Wisconsin—Madison, 1225 W. Dayton St., Madison, WI 53706.
E-mail: don.wylie@ssec.wisc.edu

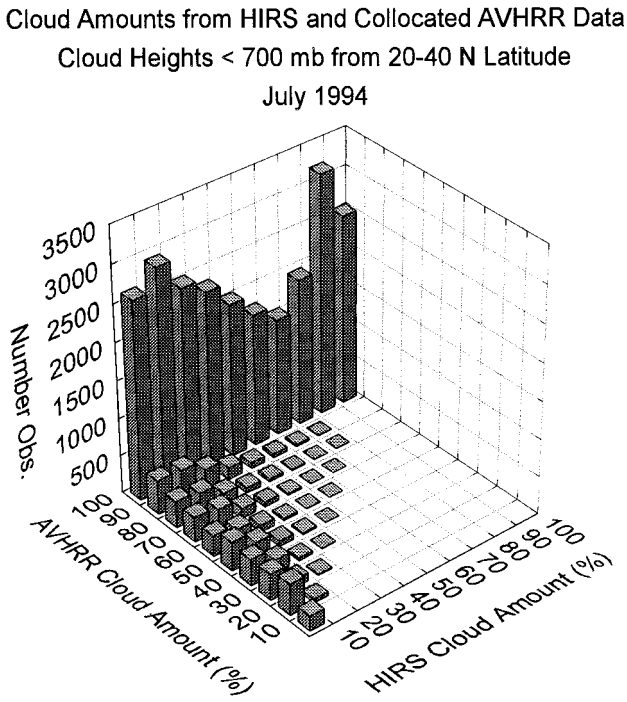

FIG. 1. AVHRR cloud coverage within a HIRS FOV plotted against HIRS effective emissivity (effective cloud amount) for clouds above 700 hPa in the tropical oceans from 20° to 40°N lat for July 1994.

Comparisons of the University of Wisconsin (UW) HIRS cloud data to other large cloud datasets have been made. Each of the other cloud studies report different frequencies of clouds because of the differences in their ability to detect clouds. In comparing the UW HIRS and ISCCP cloud data, Jin et al. (1996) note that the UW HIRS dataset reports about 12% more cloud cover due to its higher sensitivity to thin cirrus than ISCCP. Wylie and Wang (1997) describe a comparison between the HIRS and SAGE-II cloud data, finding that SAGE-II reports even more cloud cover than the UW HIRS dataset because of an even higher sensitivity to thin cirrus and a limb scanning perspective. In addition, a comparison between the ISCCP and SAGE-II cloud data can be found in Liao et al. (1995a,b). The ISCCP and UW HIRS datasets are being expanded and more comparisons are planned for future publications.

This paper builds on Wylie et al. (1994) adding more information on upper- (above 6 km) tropospheric clouds. The following sections include discussions on the geographic distributions of these clouds, as well as the densities of these clouds and geographic variances in density. Now that the dataset comprises 8 yr, a search for trends is pursued in more detail than previously undertaken. This reexamination reveals a sensitivity to individual satellite characteristics not previously noted; important lessons emerge for the development of cloud climatologies with the Earth Observing System instruments.

2. Technique

The technique for extracting cloud height and density information, along with frequency of occurrence (assumed to be synonymous with detection in this paper), from the HIRS data has been described in detail in Wylie et al. (1994). This method uses infrared radiation emanating from the earth and atmosphere in partially absorbing CO_2 channels from 13 to 15 μm. There is no appreciable solar reflection in these channels. They are spectrally positioned so that each channel detects radiation from different levels in the troposphere, hence the association of the term CO_2 slicing with this technique. The technique is based on a simplification of the radiative transfer equation that assumes the attenuation of upwelling radiation by a cloud occurs at one level in the troposphere. A more realistic depiction requires knowledge of the vertical profile of cloud density; however, since clouds come in a wide variety of vertical distributions, the single-layer assumption is the only method for obtaining a unique solution. This approach is consistent with other algorithms proposed for detecting clouds using multispectral infrared sounders (Chahine 1974; Smith et al. 1974; McCleese and Wilson 1976; Smith and Platt 1978; Wielicki and Coakley 1981; Susskind et al. 1987; Menzel et al. 1992).

Using the multispectral CO_2 channel data, the cloud level can be solved directly without knowing the infrared emissivity of the cloud or the fractional cloud cover in the field of view (Wylie et al. 1994). Assuming that the emission and absorption are identical in two spectrally close CO_2 channels, a direct calculation of the cloud level is possible in a radiative transfer formulation. Other techniques use visible channels to estimate the cloud density and emissivity with a radiative scattering model; adjustments are then made to the measured infrared window radiance (at 11 μm) for transmission through the cloud (Minnis et al. 1993a,b). CO_2 slicing does not require visible data and provides an alternate means of detecting upper-tropospheric clouds that complements the ISCCP.

In this study, HIRS CO_2 channels are used to calculate cloud levels when the cloud radiance signal, defined as the expected clear minus measured radiance for a field of view ($R_{clr} - R_m$), is greater than five times the instrument noise level ($R_{clr} - R_m > 5\sigma$); otherwise the infrared window temperature is used to determine an opaque cloud-top pressure. This assures that the measured cloud signal is safely outside of the instrument noise and indicates the presence of cloud in the CO_2 channels with a high degree of confidence. A field of view (FOV) is determined to be clear if the moisture corrected 11-μm brightness temperature is within 2.5°C of a surface temperature estimate. Over land this is inferred from the Global Data Assimilation System (Kanamitsu 1989; Parrish and Derber 1992; Parrish et al. 1997) at the National Centers for Environmental Prediction (NCEP); over the oceans this is the sea surface

TABLE 1. Cloud types found in UW HIRS study between 65°N and 65°S lat in summers and winters during Jun 1989–Feb 1997.

	Summer (Jun, Jul, and Aug)				Winter (Dec, Jan, and Feb)			
	All clouds	Thin (N $\varepsilon < 0.5$) ($\tau_{vis} < 1.4$)	Thick (N $\varepsilon \geq 0.5$) ($\tau_{vis} > 1.4$)	Opaque (N $\varepsilon > 0.95$) ($\tau_{vis} > 6$)	All clouds	Thin (N $\varepsilon < 0.5$) ($\tau_{vis} < 1.4$)	Thick (N $\varepsilon \geq 0.5$) ($\tau_{vis} > 1.4$)	Opaque (N $\varepsilon > 0.95$) ($\tau_{vis} > 6$)
>6 km	34%	15%	14%	5%	34%	15%	15%	4%
3–6 km	26	11	9	6	32	11	11	10
<3 km	45	0	0	45	47	0	0	47
All levels	73	22	20	31	76	23	21	32

temperature analysis from the National Environmental Satellite Data and Information Service (NESDIS). Temperature errors (defined by the root-mean-square differences between in situ data and the existing analysis values) are between 1 and 3 K. No surface temperature changes nor trends have been found during the course of this 8-yr cloud analysis; it can be concluded that surface temperature did not cause any trends in UW HIRS cloud study.

HIRS data from *NOAA-10, -11, -12,* and *-14* are sampled to include only data from every third FOV on every third line with a zenith angle less than 10°. With two satellites, about one-half of the earth is sampled each day. Morning orbits (0000–1200 LT) over land are rejected because a good estimate of the morning land surface temperature is unavailable, which makes discerning cloudy from clear FOVs difficult. In multiple cloud layers, the height and emissivity of a single cloud layer best representing the radiative mean of the cloud scene is estimated.

After the cloud level has been determined, the cloud effective emissivity in the 11-μm window is estimated from the ratio of the radiance signal of the measured cloud with the radiance signal of an opaque cloud at the calculated cloud level. The cloud effective emissivity is the product of cloud emissivity, ε, and the fraction of cloud coverage in the FOV, N. Since it is calculated with a radiance measured from a 20-km diameter FOV, when the cloud effective emissivity, $N\varepsilon$, is less than unity, HIRS may be observing broken cloud ($N < 1$, $\varepsilon = 1$), overcast transmissive cloud ($N = 1$, $\varepsilon < 1$), or broken transmissive cloud ($N < 1$, $\varepsilon < 1$). All of these possibilities imply an observation where the HIRS radiometer detects radiation from below a cloud layer as well as radiation from the cloud-layer top. All observations where $N\varepsilon < 0.95$ are labeled as transmissive or ''cirrus'' in this paper; those where $N\varepsilon > 0.95$ are considered to be opaque clouds.

To evaluate which component of $N\varepsilon$, cloud fraction or emissivity, is dominant, Wylie et al. (1994) presented a comparison of $N\varepsilon$ calculated with CO_2 slicing of the 20-km HIRS data to N inferred from 1-km Advanced Very High Resolution Radiometer (AVHRR) data within the HIRS FOV. When $N\varepsilon > 0.50$, all of the HIRS FOVs were entirely cloud covered ($N_{AVHRR} = 1.0$). For thinner clouds, $N\varepsilon < 0.5$, N_{AVHRR} was always greater than $N\varepsilon$. A larger study has been completed using 4-km AVHRR GAC data. N_{AVHRR} was evaluated for all *NOAA-12* HIRS FOVs in July 1994 within 20°–40° lat over ocean. Figure 1 shows N_{AVHRR} plotted against $N\varepsilon$ for clouds above 700 hPa, where N_{AVHRR} was determined using the visible and infrared screening described in Frey et al. (1996). For $N\varepsilon > 0.5$ (thick clouds), all HIRS FOVs were found to be completely cloud covered ($N_{AVHRR} = 1.0$), similar to the results in Wylie et al. (1994). For thinner clouds ($N\varepsilon < 0.5$), there was a variety of cloud coverage that had an average N_{AVHRR} of 0.72 within HIRS FOVs. To summarize, this work indicates that $N\varepsilon$ represents ε entirely when $N\varepsilon \geq 0.5$ (optically thicker clouds); otherwise, the contributions of N and ε are approximately equal (optically thinner clouds with $N\varepsilon < 0.5$). Estimates of cloud cover assume total FOV cloud obscuration when $N\varepsilon \geq 0.5$, and 72% cloud obscuration of the FOV when $N\varepsilon < 0.5$.

The calculation of effective emissivity does not account for IR scattering into the FOV. According to the model of Platt and Stephens (1980), scattered radiation could raise $N\varepsilon$ by 0.1 over the value determined for absorption only. Scattering, and hence an increase in $N\varepsilon$, is most likely for moderately transmissive clouds with $N\varepsilon \simeq 0.5$; very thin ($N\varepsilon \simeq 0.0$) and very dense clouds ($N\varepsilon \simeq 1.0$) will have little scattered radiation in the HIRS FOV.

Cloud optical depths can be estimated from the effective emissivity ($N\varepsilon$) derived from the HIRS data. By assuming that transmission is the complement of emission without scattering, the infrared window optical depth is given by

$$\tau_{IRW} = -\ln(1 - N\varepsilon). \quad (1)$$

Visible optical depths (τ_{vis}) can be estimated from infrared window optical depths. Theoretical models of radiative scattering, reinforced by lidar and satellite measurements, indicate that the optical depth in the visible is about twice that at 11 μm (Platt 1979; Platt et al. 1987; Minnis et al. 1990; Wylie et al. 1995). In this work, it is assumed that

$$\tau_{vis}/\tau_{IRW} \cong 2. \quad (2)$$

3. Geographical cloud distributions

The statistical summary of over 60 million cloud observations from HIRS between June 1989 through February 1997 is shown in Table 1. The statistics are sep-

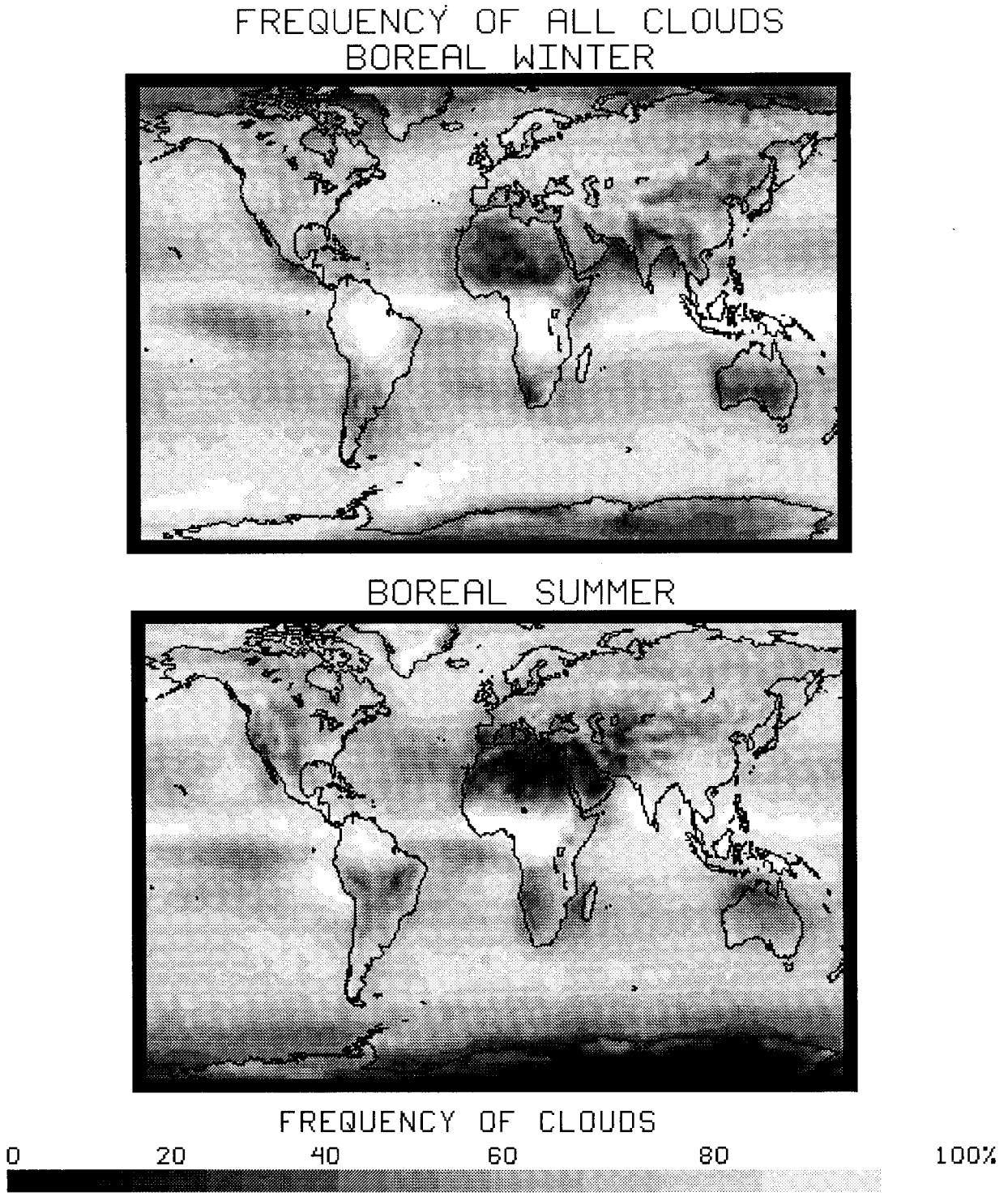

FIG. 2. The frequency of cloud detection in a HIRS FOV from 1989 to 1997. The boreal winter includes the months of Dec–Feb and the boreal summer includes the months of Jun–Aug. Eight winters and summers were averaged together.

arated by cloud type into clear sky ($\tau_{vis} < 0.1$), thin ($\tau_{vis} < 1.4$), thick ($\tau_{vis} > 1.4$), and opaque ($\tau_{vis} > 6$) clouds and separated by level in the atmosphere above 6 km, between 3 and 6 km, and below 3 km. The frequency of cloud observations in a given level of the atmosphere in Table 1 are the percentages of only observations to that level; this is different from the percentage of all observations (as presented in Wylie et al. 1994). On the

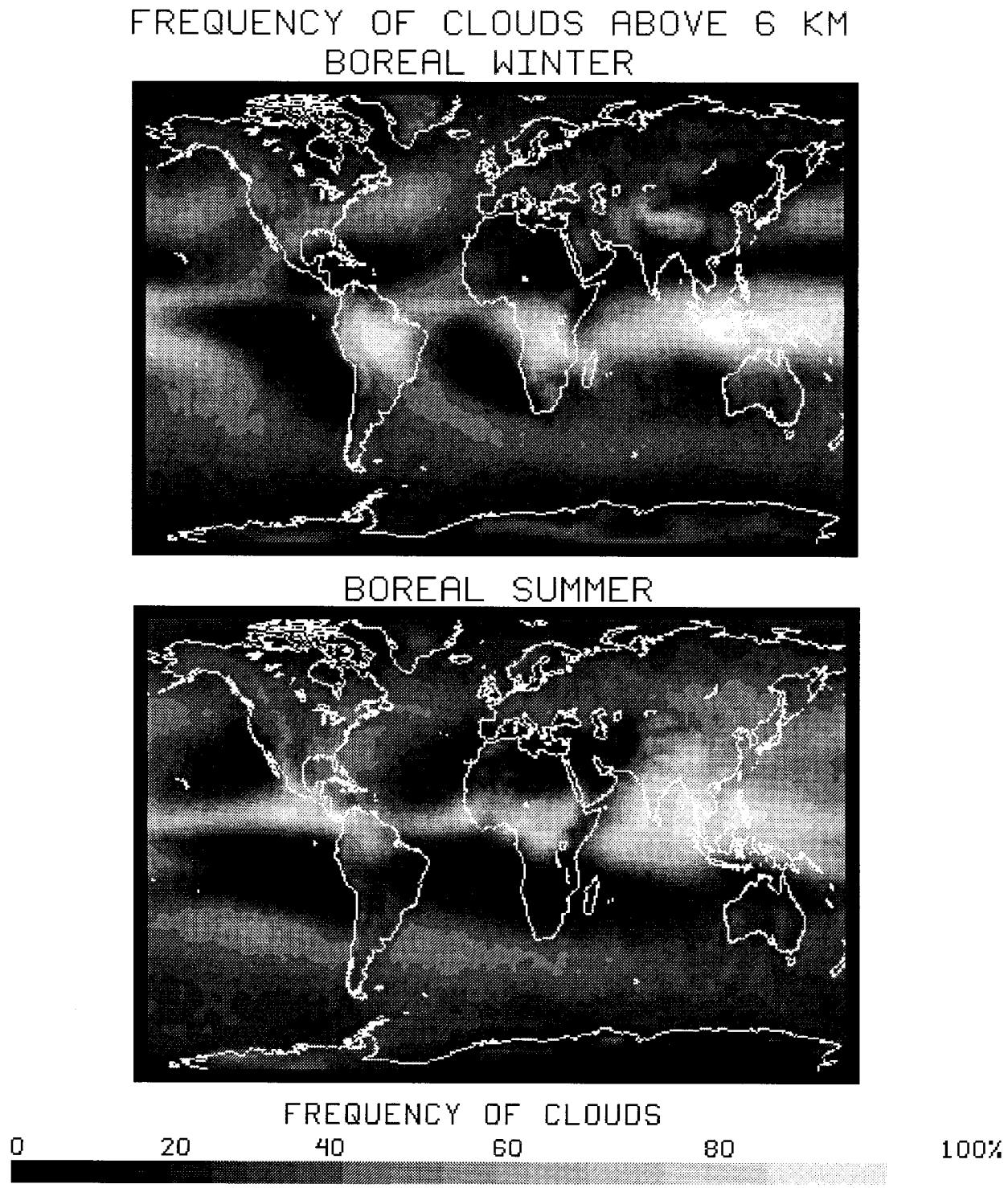

FIG. 3. The frequency of high (above 6 km) cloud detection in a HIRS FOV from 1989 to 1997.

average for summer and winter, HIRS finds thin clouds in 22% of all observations, thick clouds in 21%, and opaque clouds in 32%. From section 2, thin clouds cover 72% of the HIRS FOV on average and thick and opaque clouds cover 100%. Thus these HIRS observations imply that clouds cover about 69% of the earth from 65°S to 65°N lat. This estimate of cloud cover is believed to be valid within 3% (Menzel et al. 1992).

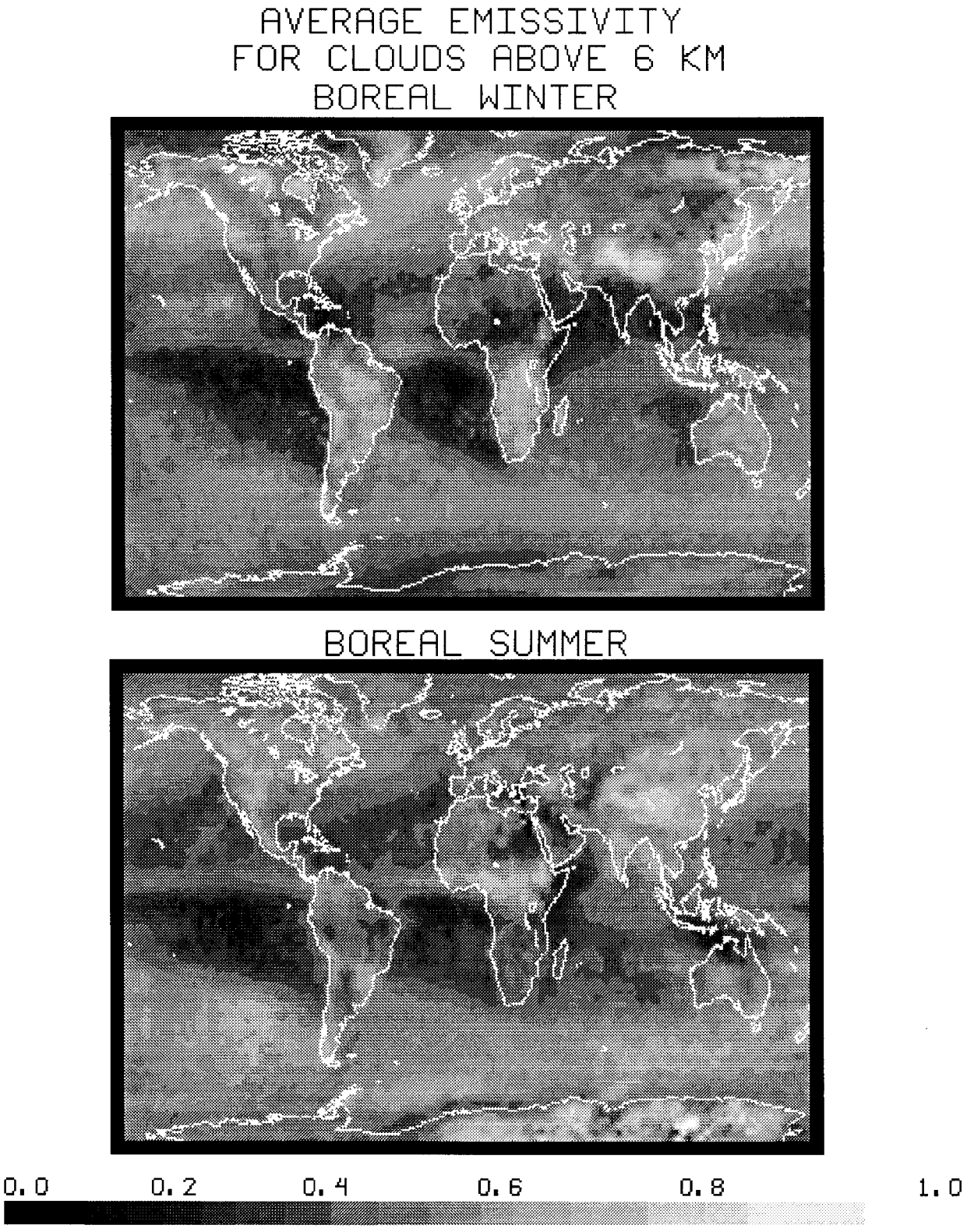

FIG. 4. The mean $N\varepsilon$ derived from the HIRS data from 1989 to 1997.

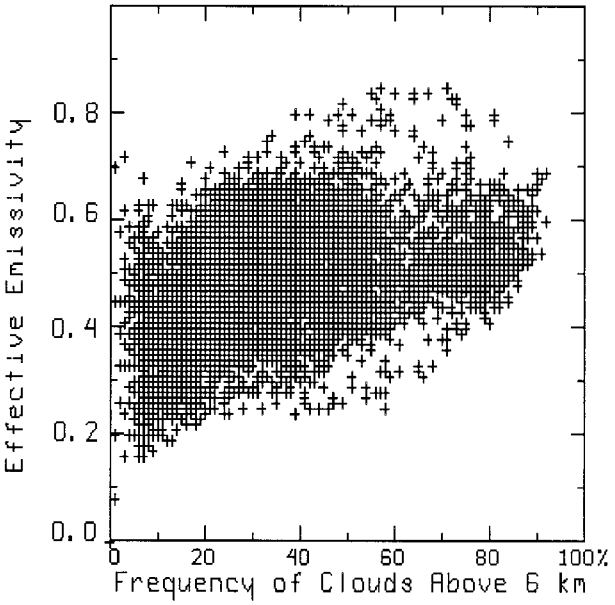

FIG. 5. The $N\varepsilon$ vs the frequency of clouds above 6 km.

Little variation is found in the boreal summer versus winter cloud statistics; clear skies are found in 27% of all observations in the boreal summer and only in 24% in the boreal winter. High clouds above 6 km are evident in 34% of the observations; 6 km roughly corresponds to 490 hPa in the Tropics and 450 hPa at 50° lat. Summer to winter, 26%–32% of the observations at midlevels between 3 and 6 km found clouds; 3 km roughly corresponds to 700 hPa in the Tropics and 685 hPa at 50° lat. Observations at low levels below 3 km found clouds 45%–47% of the time. Cirrus and transmissive clouds (with effective emissivities less than 0.95) were found in 42%–44% of all observations. All clouds below 3 km are designated as opaque because the CO_2 algorithm is not capable of resolving cloud fraction and emissivity low in the troposphere. Many of the midlevel transmissive observations are most likely broken clouds.

Figure 2 shows the geographical distribution of all clouds in the summer and winter seasons (lighter regions indicate more frequent cloud detection). The months of December–February represent the boreal winter (austral summer) and the months of June–August represent the boreal summer (austral winter). The seasonal summaries are compiled using a uniformly spaced grid of 2° lat × 3° long. Each grid box for each season has at least 1000 observations. The major features of the 8-yr summary have not changed appreciably from those reported in the 4-yr summary (Wylie et al. 1994). The intertropical convergence zone (ITCZ) is readily discernible as the region of more frequent clouds (white band in the Tropics); the midlatitude storm belts are also evident. The ITCZ is seen to move north with the sun from boreal winter to summer. The subtropical high pressure systems are seen in the regions of less frequent cloud cover. Over the Indonesian region the ITCZ expands in latitudinal coverage from boreal winter to summer. In the central Pacific Ocean, the ITCZ shows both a southern and northern extension during the boreal winter months. In the Southern Hemisphere, the eastern Pacific Ocean off South America and the eastern Atlantic Ocean off Africa remain relatively free of clouds throughout the year. The Southern Hemispheric storm belt is evident throughout the year. In the Northern Hemisphere's midlatitude storm belts, the frequency of clouds increases during the winter with the strengthening of the Aleutian low in the North Pacific Ocean and the Icelandic low in the North Atlantic Ocean. The North American cloud cover shows little seasonal change. Large convective development occurs during the austral summer (boreal winter) in South America and Africa, which is readily apparent in the increased detection of clouds.

Some regions exhibit cloudy conditions for a complete season. In two grid boxes in the African ITCZ (8°N, 10.5°W and 2°N, 19.5°E), all HIRS observations found cloud during all boreal summers of this study. Eight grid boxes were cloudy for all boreal winters of this study; four were located in the central Amazon (centered at 8°S, 58°W), two in the African Congo (6°S, 26°E), and two in the Indonesian area (2°S, 113°E and 4°S, 146°E). With each grid box covering approximately 75 000 km^2, in the boreal winter there are about 300 000 km^2 in the Amazon that are always cloud covered. There were no grid boxes where all HIRS observations found cloud in all seasons.

Observations of clouds above 6 km (Fig. 3) exhibit the same general geographical patterns found for total clouds in Fig. 2. They are most predominant in the tropical ITCZ and move with the seasons. During the boreal winter in a few areas such as southern Brazil, tropical South Africa, and Indonesia, high clouds are found in more than 90% of the observations. Less frequent occurrence is found in the midlatitude storm belts. Differences in observations of high clouds and observations of all clouds are evident in the subtropical highs over the extratropical oceans where marine stratus clouds are prevalent and higher clouds are far less frequent. This is evident along the west coasts of North and South America and Africa.

Comparison with ISCCP data reveals that the UW HIRS multispectral analysis is finding roughly twice as many transmissive clouds than the ISCCP visible and infrared window analysis. Jin et al. (1996) studied collocated ISCCP and HIRS data for four months (July 1989, October 1989, January 1990, and April 1990). HIRS finds cloud in 76% of its observations and ISCCP finds cloud in 63%; the HIRS detection of thin clouds (17% compared to 7% for ISCCP) accounts for most of this difference. Jin et al. (1996) note a lower number of UW HIRS reports of cloud in mountainous areas due to a cold bias in the surface temperatures used in the UW algorithm. In one year (March 1985–February 1986) of ISCCP data, Hartmann et al. (1992) find sem-

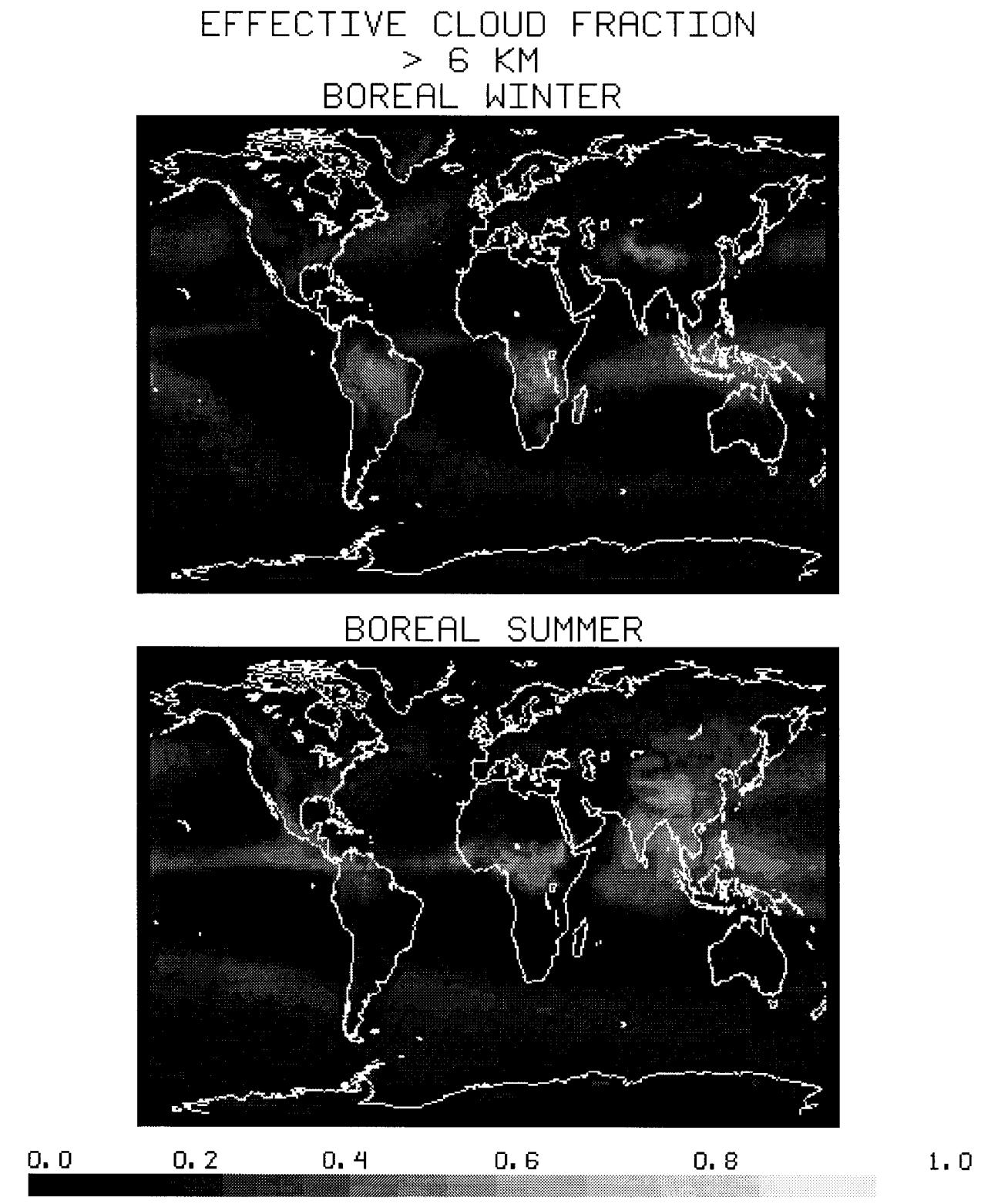

FIG. 6. The mean CF_6 for clouds above 6 km derived from the HIRS data from 1989 to 1997.

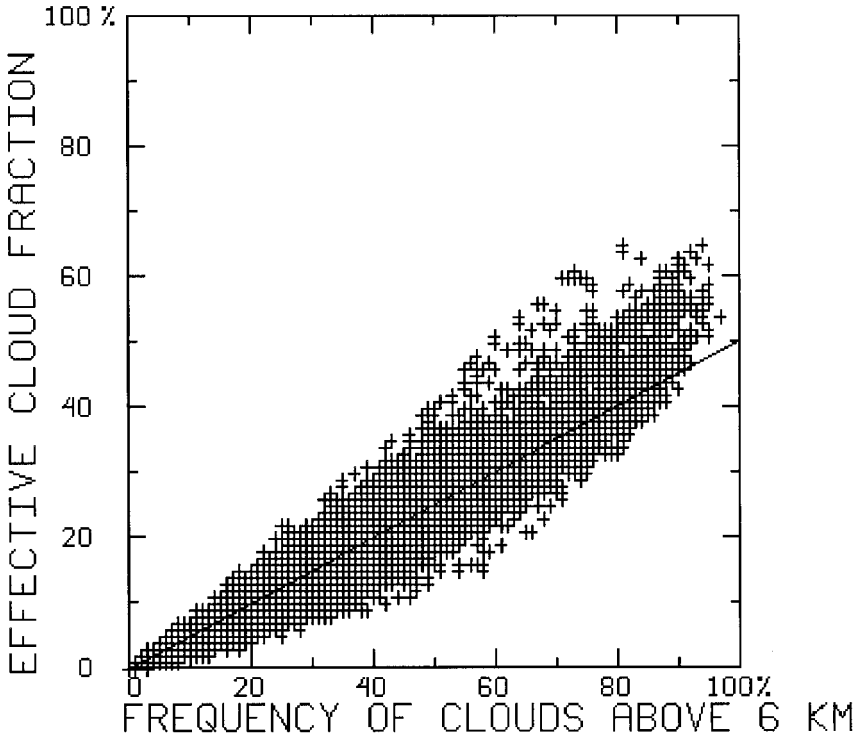

FIG. 7. The CF_6 vs the frequency of clouds above 6 km.

itransparent clouds (visible optical depth less than 9.4) 21% of the time; HIRS finds 44% in the 8 yr of this study (June 1989–May 1993). These comparisons point to the ISCCP difficulty in detecting thin transmissive clouds; if one were to exclude clouds with $\tau_{vis} < 1.4$ from the HIRS data (roughly 20% of the observations) and increase the frequency of low opaque clouds in the HIRS data (adding roughly 5%), all adjusted HIRS cloud categories would agree with Jin et al. (1996) and Hartmann et al. (1992) to within a few percent.

Comparison with SAGE II data from the summers of 1989 and 1990 and the winters of 1990 and 1991 (Wylie and Wang, 1997) reveals good correlation (greater than 0.8) in the geographical distribution of clouds above 5 km. This must be considered in the context of the differing observing characteristics of the two systems (SAGE limb scanning over 2.5 × 200 km FOVs versus HIRS nadir 20-km FOVs); in addition SAGE can detect clouds with $\tau_{vis} \geq 0.0002$ whereas HIRS is sensitive to clouds when $\tau_{vis} \geq 0.1$. There is good comparison of the percentage of observations that find clouds in the winter hemispheres and the Tropics (within 5%), but in the summer hemispheres SAGE finds more clouds (up to 15%). On the average, 87% of the SAGE observations found cloud in 1989 and 1990, whereas 76% of the HIRS observations found cloud; SAGE is expected to find more clouds given its limb scanning and larger FOV. Overall, the similarities in these two cloud datasets are encouraging.

4. Cloud densities

The effective emissivities derived from the CO_2 slicing analysis are shown in Fig. 4. They show the same basic geographical distributions as the frequencies of high clouds (Fig. 3), but the spatial gradients are less distinct. The ITCZ and midlatitude storm belts have the highest effective emissivities, averaging about 0.6. The subtropical high and subtropical desert regions have smaller values, averaging between 0.2 and 0.3. The effective emissivities are partially correlated with frequency of high cloud; a correlation of 0.30 is found in the boreal winter and 0.35 in the boreal summer (see scatterplots in Fig. 5). The average effective emissivity is 0.51 (in both winter and summer), which can be equated with $\tau_{vis} = 1.4$ using Eqs. (1) and (2). Most of the clouds above 6 km have visible optical depths between 0.5 to 1.8 (effective emissivities between 0.2 and 0.6).

For calculating energy budgets, the frequencies of cloud observation have to be considered along with the cloud effective emissivities. Within each HIRS FOV, $N\varepsilon$ is dominated by the ε, as discussed in section 2. Within the grid box of these cloud summaries (2° lat × 3° long), N is expected to be a larger factor in the radiative transfer calculations than ε. The summary grid box is between 100 to 180 times larger than the HIRS FOV. To account for this, the $N\varepsilon$ is combined with the cloud frequency above 6 km (F_6) to form an effective cloud fraction (CF_6) over the grid box, so that

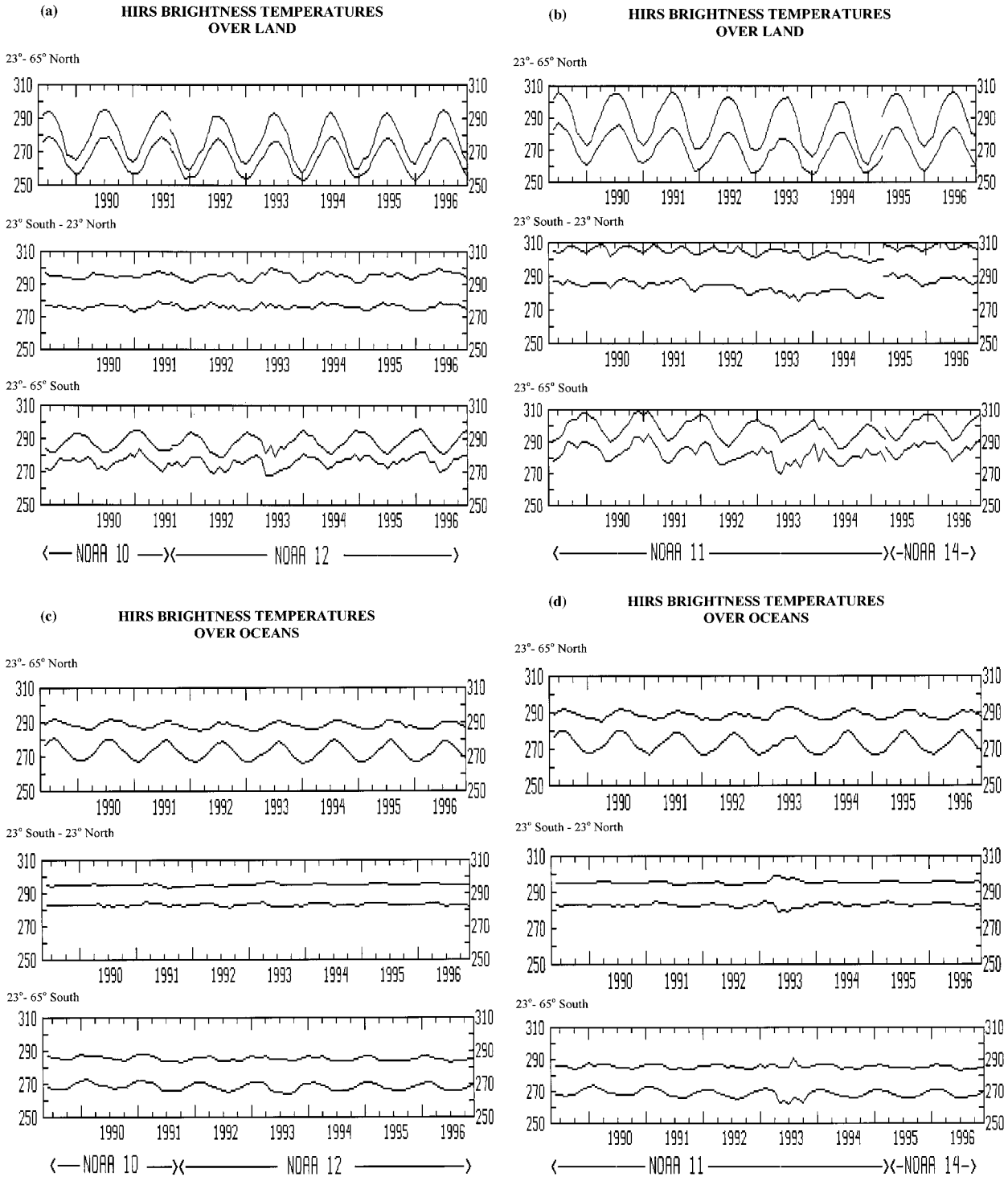

FIG. 8. (a) Monthly averages of the HIRS 11-μm window channel data over land for the sunrise and sunset satellites, *NOAA-10* and *-12*. The lower line is the average of all HIRS data and the upper line is the average of all HIRS FOVs declared clear by the algorithm's cloud mask. (top) Averaged over 23°–65°N lat. (middle) Averaged over the Tropics from 23°S to 23°N lat. (bottom) Averaged over 65°–23°S lat. (b) Same as (a) for the midday and midnight satellites, *NOAA-11* and *-14*. (c) The monthly averages from *NOAA-10* and *-12* over oceans. The panels designate 23°–65°N, 23°S–23°N, and 65°–23°S as in (a) and (b). (d) Same as (c) but for *NOAA-11* and *-14*.

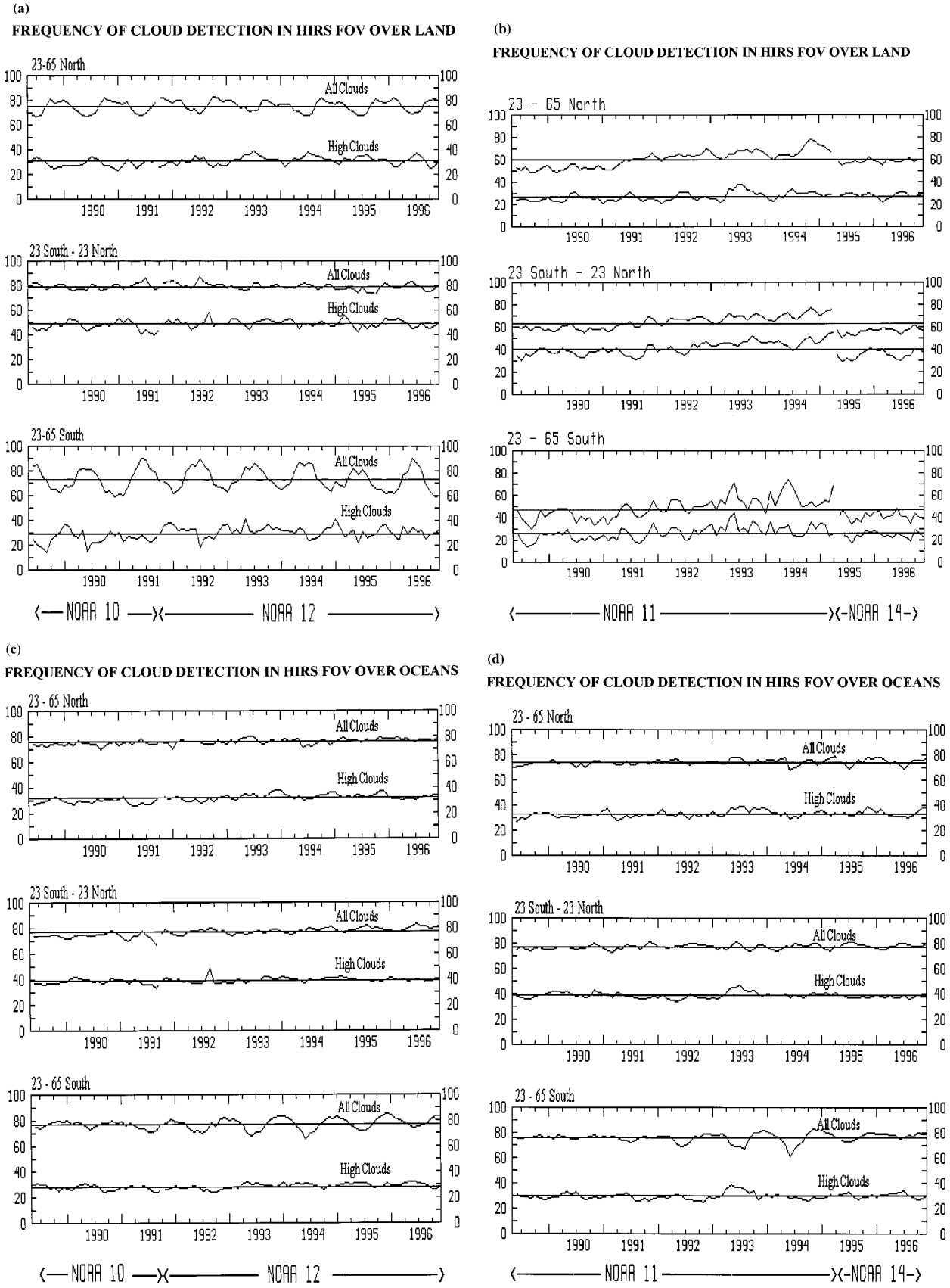
(a)
FREQUENCY OF CLOUD DETECTION IN HIRS FOV OVER LAND
23-65 North
All Clouds
High Clouds
23 South - 23 North
All Clouds
High Clouds
23-65 South
All Clouds
High Clouds
1990 1991 1992 1993 1994 1995 1996
NOAA 10
NOAA 12
(b)
FREQUENCY OF CLOUD DETECTION IN HIRS FOV OVER LAND
23 - 65 North
23 South - 23 North
23 - 65 South
1990 1991 1992 1993 1994 1995 1996
NOAA 11
NOAA 14
(c)
FREQUENCY OF CLOUD DETECTION IN HIRS FOV OVER OCEANS
23 - 65 North
All Clouds
High Clouds
23 South - 23 North
All Clouds
High Clouds
23 - 65 South
All Clouds
High Clouds
1990 1991 1992 1993 1994 1995 1996
NOAA 10
NOAA 12
(d)
FREQUENCY OF CLOUD DETECTION IN HIRS FOV OVER OCEANS
23 - 65 North
All Clouds
High Clouds
23 South - 23 North
All Clouds
High Clouds
23 - 65 South
All Clouds
High Clouds
1990 1991 1992 1993 1994 1995 1996
NOAA 11
NOAA 14

TABLE 2. The change in the frequency of cloud detection (all clouds and high clouds above 440 hPa) from Jun 1989 to Feb 1997. The change is percentage of observations that found cloud at the end of the study period minus the percentage of cloud observations at the beginning. High clouds observed by *NOAA-10–12* increased 4%–5% over land and ocean in the Northern Hemisphere; in the Tropics this is closer to 2%. In the Southern Hemisphere high clouds increased by 3% over water and by 6% over land. *NOAA-11* trends over land are problematic because of the orbit drift; *NOAA-14* trends are difficult as they cover only 1.7 yr to date.

	All clouds				High clouds			
	10/12		11/14		10/12		11/14	
Latitude belt	Mean	Inc	Mean	Inc	Mean	Inc	Mean	Inc
				Over water				
23°–65°N	75.7	+3.1	74.3	+1.7	31.6	+4.9	33.1	+3.3
Tropics	76.8	+6.6	77.5	+2.1	39.0	+1.6	38.7	−0.4
23°–65°S	77.1	+1.7	76.1	+1.5	28.4	+2.7	29.7	+1.3
				Over land				
	10/12				10/12			
	Mean		Inc		Mean		Inc	
23°–65°N	75.4		+1.1		30.6		+4.2	
Tropics	79.3		−2.1		48.5		+2.0	
23°–65°S	73.5		−2.0		29.4		+6.2	

$$\mathrm{CF}_6 = F_6 N\varepsilon, \tag{3}$$

where CF_6 represents both the frequency of clouds above 6 km and their optical density. Figure 6 shows that CF_6 geographical distributions are similar to those of F_6 (Fig. 3). The relationship between CF_6 and F_6 appears to be nearly linear (Fig. 7), with a correlation of 0.96. Up to $F_6 \approx 50\%$, $\mathrm{CF}_6 \approx 0.5\ F_6$; for $F_6 > 50\%$, $\mathrm{CF}_6 \approx 0.6\ F_6$. This implies that the mean $N\varepsilon$ is about 0.5 in most areas, except where higher cloud frequencies occur ($F_6 > 50\%$); in this case the mean $N\varepsilon$ is about 0.6.

5. Time trends

Wylie et al. (1994) reported a possible increase in the observation of upper-tropospheric clouds. As the HIRS record has grown to eight years and evolved to four satellites, the changes over time in the HIRS data have been reexamined in greater detail. The monthly averages of infrared window brightness temperature and cloud frequency (total and high) have been investigated for each satellite. Oceanic data were distinguished from the land data. These time series are shown in Figs. 8 and 9.

As discussed in section 2, the UW HIRS cloud study uses surface temperature data to distinguish clear HIRS FOVs. Since the CO_2 algorithm requires a clear radiance value for each channel at each location (Wylie et al. 1994), clear radiances must be inferred from nearby clear FOV measurements or calculated where the temperature structure of the atmosphere is well known. Given the likelihood of biases in the radiances calculated from temperature data in the global model analysis, we measure radiances in known clear FOVs and interpolate these values into the cloudy areas. The cloud mask compares the moisture-corrected HIRS 11-μm radiance blackbody temperature to surface temperature measurements or estimates; the cloud mask then decides if the FOV is clear or possibly cloudy. Corrections for water vapor attenuation are made using the moisture sensitive HIRS channel at 8.3 or 12.7 μm. Tests of the cloud mask show that lowering the surface temperature by 2 K causes 15% of the HIRS FOVs, which are mostly thin cirrus, to be labeled as clear. Realizing the sensitivity of the UW HIRS cloud data to surface temperatures, we examined our temperature data for possible trends and found none.

The surface temperature data used in the UW HIRS cloud study do not show any trend over land or water. The HIRS infrared window channel measurements are shown in Fig. 8. The warmer temperature plot is the monthly average of the clear only HIRS FOVs, whereas the colder plot is the average of all clear and cloudy HIRS FOVs. There are two satellites and three latitude belts shown in each of Figs. 8a, 8b, 8c, and 8d; Figs. 8a and 8b show data over land and 8c and 8d show data over oceans. *NOAA-10* and *-12* are the sunrise and sunset operational satellites, and *NOAA-11* and *-14* are the midday and midnight satellites. Each NOAA satellite is in a sun-synchronous orbit, which attempts to sample an area twice per day at the same local solar times. *NOAA-10* and *-12* are intended to have overpass times of 0800 and 2000 LT and *NOAA-11* and *-14* have target

←

FIG. 9. (a) The frequency of all clouds (upper line) and high clouds above 440 hPa (lower line) over land for the sunrise and sunset satellites, *NOAA-10* and *-12*. The three panels are for latitude belts of 23°–65°N, 23°S–23°N, and 65°–23°S as in Fig. 8. (b) The cloud frequencies over land for the midday and midnight satellites *NOAA-11* and *-14*. (c) The cloud frequencies over water for sunrise and sunset satellites *NOAA-10* and *-12*. (d) The cloud frequencies over water for the midday and midnight satellites *NOAA-11* and *-14*.

times of 0200 and 1400 LT. Seasonal cycles are obvious over land, especially in the Northern Hemisphere. Winter to summer changes of 20–30 K are apparent. Over oceans, a weaker seasonal cycle is found. The seasonal cycle is strongest in the Northern Hemisphere and barely visible in the Southern Hemisphere. The Tropics do not exhibit any seasonal cycle over oceans and only a very weak cycle over land. These characteristics were expected.

Some problems were encountered as the *NOAA-11* orbit changed. *NOAA-11* regressed 2.5 h in local solar time from 1989 to 1995. As land cools in the afternoon, this caused an unexpected decrease of 7–12 K in the *NOAA-11* HIRS brightness temperatures over land. The drift in the *NOAA-11* orbit to later in the afternoon also increased the reported frequency of clouds over land. All cloud forms increased by 16%–21% (percentage of all observations both clear and cloudy) whereas high clouds increased by 7%–15%. These were probably low broken clouds and thin cirrus with $N\varepsilon \ll 1.0$. Over oceans, *NOAA-11*'s orbit change did not affect the monthly average HIRS brightness temperatures or frequency of cloud reports.

Another anomaly appeared April–June 1993 when *NOAA-11* occasionally reported unrealistically large window channel brightness temperatures. These temperatures were often 20 K larger than the SST in the Tropics and the Southern Hemisphere (Fig. 8d). These anomalous window channel temperatures are now screened out; any HIRS temperatures 5 K greater than the SST or 20 K greater than the land temperature are discarded.

A final difficulty was found in the determination of clear-sky radiances. As indicated in section 2, the UW HIRS cloud study restricted investigation of clouds to data with HIRS scan angles less than 10° from nadir in an attempt to study clouds from a top down view (rather than a side view) and to mitigate the effect of increased pathlength through the atmosphere on transmittance calculations (as seen in limb darkening). However for June 1989 to May 1991, data from scan angles up to 25° were used to infer the clear-sky radiances in the cloudy FOVs while cloud properties were calculated only for data from scan angles less than 10°. Thus the clear-sky radiances included some limb darkening effects (less radiance detected), whereas the cloudy sky radiances did not. The effect was to decrease the frequency of cloud reports by 1% when clear-sky radiances included some limb darkened (out to 25°) radiances. High clouds were decreased by 3%. In May 1991, scan angles were restricted to less than 10° for all processing (both clear and cloudy FOVs). Adjustments to the UW HIRS cloud trend statistics have been made so that all cloud reports (before and after May 1991) refer to data within 10° of nadir. The effects of sensor scan angle on cloud frequency statistics are discussed in further detail in the appendix.

To search for trends in cloud cover, monthly averages of the cloud frequencies were calculated for each satellite and plotted as one continuous record (see Fig. 9). *NOAA-12* replaced *NOAA-10* in September 1991, and *NOAA-14* replaced *NOAA-11* in April 1995. Cloud frequency trends over land are credible only for *NOAA-10* and *-14* (Fig. 9a), as the changes in the *NOAA-11* orbit confuse the trends over land for the midday and midnight times (Fig. 9b). When *NOAA-14* replaces *NOAA-11* and HIRS observations resume at the nominal slots in the diurnal cycle (0200 and 1400LT), there is a noticeable decrease in the frequency of HIRS detection of cloud over land. The trends over ocean (Fig. 9c and 9d) reveal that an annual cycle of all clouds over oceans becomes noticeable in 1993 in the southern midlatitudes; in the Tropics and the northern midlatitudes there is little discernible change in cloud cover with the seasons. High clouds show little seasonal fluctuation anywhere. Subtle trends can be seen in the annual increase of cloud cover for all three regions.

Table 2 summarizes the changes in cloud cover during the 8 yr of this study period inferred from a linear fit to the trends in Fig. 9. Over oceans, larger changes are evident in the *NOAA-10* and *-12* sunrise and sunset observations than in the *NOAA-11* and *-14* midday and midnight observations. *NOAA-10* and *-12* find increases in all clouds ranging from 1.7% in the southern midlatitudes to 6.6% in the Tropics. *NOAA-11* and *-14* find smaller increases from 1.5% to 2.1%. The largest increase in total cloud cover is in the Tropics. High clouds (pressure height $<$ 440 hPa) exhibit the largest changes in the northern midlatitudes where increases of 4.9 and 3.3% are found. The Tropics show minimal changes in high cloud. Over land, the *NOAA-10* and *-12* trends are very small (increases of 2% or less are found). Southern midlatitude land coverage is small and thus the apparent increase in high clouds is not considered significant. *NOAA-11* and *-14* trends over land are not included in the table; *NOAA-11* trends over land are problematic because of the orbit drift and *NOAA-14* trends are difficult as they cover only 1.7 yr to date.

6. Summary and conclusions

Clouds with optical depths $\tau_{\text{vis}} > 0.1$ cover 69% of the earth between 65°N and 65°S. High clouds are found more often in the Tropics than in the northern and southern midlatitudes, indicating the ITCZ. Large latitudinal movement in cloud cover with the changing seasons is apparent on geographical plots.

Clouds that are semitransparent in the infrared ($0.1 < \tau_{\text{vis}} < 6$) are found in 43% of the HIRS observations. These clouds have a mean effective emissivity between 0.5 and 0.6 (the larger value evident in areas of frequent cloud cover).

Annual trends are small and hard to distinguish from larger seasonal differences. There is evidence of a gradual increase in the occurrence of high clouds in the northern midlatitudes (0.5% yr^{-1}) and all clouds in the

Tropics (0.8% yr^{-1}); the southern midlatitudes show very little change in cloud cover of any type during this study.

The UW HIRS cloud datasets are available for further study at http://www.ssec.wisc.edu/~donw.

Acknowledgments. The authors wish to acknowledge the contributions from several colleagues. Mr. Richard Frey studied the relative contributions of cloud fraction or cloud emissivity with AVHRR and HIRS data. Mr. Harold Woolf contributed many hours toward maintaining reliable access to the HIRS data used in this study; Mr. Geary Callan acquired the necessary ancillary data to complete the dataset for cloud studies. Ms. Kathy Strabala compiled many of the cloud datasets for investigating geographical and temporal trends and contributed to many lively discussions of the results. This work was supported by the National Environmental Satellite Data and Information Service of the National Oceanic and Atmospheric Administration (NOAA/NESDIS), which provided the HIRS data and support under Contract 50-WCNE-8-06058. Additional support came from Grants N00014-85-K-0581 and N00014-87-K-0436 from the Office of Naval Research; Grants NAG1-553 and NAG1-1830 and Contract NAS5-31367 from the National Aeronautics and Space Administration; Grant ATM-8703966 from the National Science Foundation; and Grant F19628-91-K-0007 from the United States Air Force Geophysics Laboratory.

APPENDIX

The Effects of Sensor Scan Angle on Cloud Frequency Statistics

For the UW HIRS cloud study, the HIRS data have been restricted to within 10° of nadir in order to maintain top down sensing of clouds. Viewing out to larger scan angles increases the likelihood of sensing clouds and necessitates corrections for increased pathlength through the atmosphere in the radiative transfer equation. Fifteen days of data from April 1997 are processed in three different ways to investigate the effects of sensor scan angle on cloud frequency statistics. The control run uses only data within 10° of nadir, which is the method used in this work. The second run includes HIRS data out to 25° of nadir. The third run includes all HIRS data out to scan angles of 59°, which is near the limit of the HIRS scan. All three runs use *NOAA-12* and *-14* data collected globally from 65°N to 65°S, both over land and water.

The data processing has several steps. Clear HIRS FOVs are identified first; these are then interpolated to estimate clear radiance values at each cloudy FOV. Measured cloud signal is then compared to calculated cloud signal for a given FOV where the calculated cloud signal uses transmittances adjusted for the scan angle of that FOV. When clear FOVs from a range of scan angles are used, the interpolated clear-sky radiances often include limb-darkening effects inappropriate to the scan angle of the given cloud FOV. The data from angles other than nadir measure slightly lower radiances and brightness temperatures because each CO_2 channel receives radiation from higher levels in the troposphere than the nadir FOVs. The inclusion of clear FOVs out to 25° from nadir lowers the average brightness temperature of the CO_2 channels by 0.3 K with respect to the average brightness temperature from clear FOVs within 10° of nadir. This difference is very small but significant for cloud studies.

TABLE A1. Frequency of HIRS cloud detection for 15 days in April 1997 using different scan angles.

Test run	Freq. all clouds	Freq. high clouds
≤10° scan	76.7%	29.9%
≤25° scan	79.5%	31.2%
≤59° scan	84.9%	35.9%

Global statistics show differences due to the scan angle. The results of the three runs are shown in Table A1. Cloud detection increases from 76.7% for data from scan angles <10° to 84.9% for data with angles <59° (the full swath). High clouds increase from a reported 29.9% for <10° to 35.9% for <59°.

REFERENCES

Chahine, M. T., 1974: Remote sounding of cloudy atmospheres. Part I: The single cloud layer. *J. Atmos. Sci.,* **31,** 233–243.

Frey, R. A., and S. A. Ackerman, 1996: Climate parameters from satellite spectral measurements. Part I: Collocated AVHRR and HIRS/2 observations of spectral greenhouse parameter. *J. Climate,* **9,** 327–344.

Gruber, A., and T. S. Chen, 1988: Diurnal variation of outgoing longwave radiation. *J. Climate Appl. Meteor.,* **8,** 1–16.

Hartmann, D. L., M. E. Ockert-Bell, and M. L. Michelsen, 1992: The effect of cloud type on the earth's energy balance: Global analysis. *J. Climate,* **5,** 1281–1304.

Jin, Y., W. B. Rossow, and D. P. Wylie, 1996: Comparison of the climatologies of high-level clouds from HIRS and ISCCP. *J. Climate,* **9,** 2850–2879.

Kanamitsu, M., 1989: Description of the NMC global data assimilation and forecasting system, *Wea. Forecasting,* **4,** 334–342.

Liao, X., W. B. Rossow, and D. Rind, 1995a: Comparison between SAGE II and ISCCP high-level clouds. Part 1: Global and zonal mean cloud amounts. *J. Geophys. Res.,* **100,** 1121–1135.

——, ——, and ——, 1995b: Comparison between SAGE II and ISCCP high-level clouds. Part II: Locating cloud tops. *J. Geophys. Res.,* **100,** 1137–1147.

McCleese, D. J., and L. W. Wilson, 1976: Cloud top height from temperature sounding instruments. *Quart. J. Roy. Meteor. Soc.,* **102,** 781–790.

Menzel, W. P., D. P. Wylie, and K. I. Strabala, 1992: Seasonal and diurnal changes in cirrus clouds as seen in four years of observations with the VAS. *J. Appl. Meteor.,* **31,** 370–385.

Minnis, P., D. F. Young, K. Sassen, J. M. Alvarez, and C. J. Grund, 1990: The 27–28 October 1986 FIRE IFO cirrus case study: Cirrus parameter relationships derived from satellite and lidar data., *Mon. Wea. Rev.,* **118,** 2402–2425.

——, K. N. Liou, and Y. Takano, 1993a: Inference of cirrus cloud properties using satellite-observed visible and infrared radiances.

Part I: Parameterization of radiance fields. *J. Atmos. Sci.,* **50,** 1279–1304.

——, P. W. Heck, and D. F. Young, 1993b: Inference of cirrus cloud properties using satellite-observed visible and infrared radiances. Part II: Verification of theoretical cirrus radiative properties. *J. Atmos. Sci.,* **50,** 1305–1322.

Parrish, D. F., and J. C. Derber, 1992: The National Meteorological Center's spectral statistical interpolation analysis. *Mon. Wea. Rev.,* **8,** 1747–1763.

——, ——, J. Purser, W. Wu, and Z. Pu, 1997: The NMC Global Analysis System: Recent improvements and future plans. *J. Meteor. Soc. Japan,* **75,** 359–365.

Platt, C. M. R., 1979: Remote sounding of high clouds. Part I: Calculation of visible and infrared optical properties from lidar and radiometric measurements. *J. Appl. Meteor.,* **18,** 1130–1143.

——, and G. L. Stephens, 1980: The interpretation of remotely sensed high cloud emittances. *J. Atmos. Sci.,* **37,** 2314–2321.

——, J. C. Scott, and A. C. Dilley, 1987: Remote sounding of high clouds. Part VI: Optical properties of midlatitude and tropical cirrus. *J. Atmos. Sci.,* **44,** 729–747.

Rossow, W. B. and R. A. Schiffer, 1991: ISCCP cloud data products. *Bull. Amer. Meteor. Soc.,* **72,** 2–20.

Smith, W. L., and C. M. R. Platt, 1978: Intercomparison of radiosonde, ground based laser, and satellite deduced cloud heights. *J. Appl. Meteor.,* **17,** 1796–1802.

——, H. M. Woolf, P. G. Abel, C. M. Hayden, M. Chalfant, and N. Grody, 1974: *Nimbus 5* sounder data processing system. Part I: Measurement characteristics and data reduction procedures. NOAA Tech. Memo. NESS 57, 99 pp.

Stowe, L., G. G. Wellemeyer, T. F. Eck, H. Y. M. Yeh, and the *Nimbus-7* Cloud Data Processing Team, 1988: *Nimbus-7* global cloud climatology. Part I: Algorithms and validation. *J. Climate,* **1,** 445–470.

Susskind, J., D. Reuter, and M. T. Chahine, 1987: Clouds fields retrieved from HIRS/MSU data. *J. Geophys. Res.,* **92,** 4035–4050.

——, P. Piraino, L. Rokke, L. Iredell, and A. Mehta, 1997: Characteristics of the TOVS pathfinder path A dataset. *Bull. Amer. Meteor. Soc.,* **78,** 1449–1472.

Warren, S. G., C. J. Haln, J. London, R. M. Chervin, R. L. Jenne, 1988: Global distribution of total cloud over and cloud type amounts over the ocean. NCAR Tech. Note TN-317+STR, National Center for Atmospheric Research, Boulder, CO, 212 pp. [Available from UCAR Publications, P.O. Box 3000, Boulder, CO 80307.]

——, ——, ——, ——, and ——, 1986: Global distribution of total cloud cover and cloud type amounts over land. NCAR Tech Note TN-273+STR, National Center for Atmospheric Research, Boulder, CO, 209 pp. [NTIS DE87-006903.]

Wielicki, B. A., and J. A. Coakley, 1981: Cloud retrieval using infrared sounder data: Error analysis. *J. Appl. Meteor.,* **20,** 157–169.

Wylie, D. P., and W. P. Menzel, 1989: Two years of cloud cover statistics using VAS. *J. Climate,* **2,** 380–392.

——, and P. Wang, 1997: Comparison of cloud frequency data from HIRS and SAGE II. *J. Geophys. Res.,* **102,** 29 893–29 900.

——, W. P. Menzel, H. M. Woolf, and K. I. Strabala, 1994: Four years of global cirrus cloud statistics using HIRS. *J. Climate,* **7,** 1972–1986.

——, P. Piironen, W. Wolf, and E. Eloranta, 1995: Understanding satellite cirrus cloud climatologies with calibrated lidar optical depths. *J. Atmos. Sci.,* **52,** 4327–4343.